# Multistatic Target Tracking Using Specular Cue Initiation and Directed Data Retrieval

**Doug Grimmett**
SPAWAR Systems Center San Diego (SSC-SD)
53560 Hull Street, San Diego, CA, 92152-5001, U.S.A.
grimmett@spawar.navy.mil

**Abstract** - *The effective fusion and tracking of multistatic active sonar contacts is challenging, due to high levels of false alarm clutter present on all sonar nodes. Exploiting the occurrence of high strength detections generated by the specular geometric condition, a cueing approach can be used to selectively extract further data stored locally on the individual sonar nodes for ingestion into the multi-sensor, multi-target tracker. This approach can significantly reduce the data rate at the input to the fusion/tracking algorithm, and reduce node-to-fusion-center communication link throughput requirements. This paper describes this concept, its associated multistatic tracking algorithm, and provides results obtained using simulated multistatic data from the Multistatic Tracking Working Group (MSTWG). The results show effective tracking performance using this approach, yielding a single high quality target track with zero false tracks. The method is shown to have excellent potential in reducing the overloading of the communication links, the automated tracking algorithm, and the operator.*

**Keywords:** Multistatic Sonar – Multi-Sensor Fusion – Tracking – Cueing – Specular – Target Strength

## 1. Introduction

Distributed multistatic active sonar networks have the potential to increase ASW performance against small, quiet, threat submarines in the harsh clutter-saturated littoral and the deeper open ocean. This improved performance comes through the expanded geometric diversity achieved with multiple sources and receivers, and results in increased probability of detection, area coverage, target tracking, classification, and localization through cross-fixing [1].

However, with the increased number of sensors in a multistatic network, come corresponding increases in the data rate, processing, communications requirements, and operator loading. Without an effective fusion of the multistatic data, the benefits of such systems will be unrealizable. Effective, robust, and automated multi-sensor data fusion and tracking algorithms become an essential part of such systems. Much progress has recently been made in this field [2-3], however, overloading due to high false alarm rates is still a major issue. Multistatic fusion algorithms are still challenged to automatically output a sufficiently low false track/alert rate to the operator in these reverberation- and clutter-rich conditions. Communication links may not have the throughput capacity to transfer all of the associated information from the multistatic nodes to a fusion center.

A concept referred to as the "Specular-Cued Surveillance Web (SPECSweb)" is being pursued to address this data rate problem through "specular cueing", directed data retrieval, and novel fusion techniques. This approach can potentially provide a robust, automated ASW detection and tracking method, resulting in a significant reduction in false alarm rates compared to conventional multistatic fusion methods. The SPECSweb application area is ASW surveillance (not necessarily tactical) scenarios/missions. This paper shows the potential of this cueing and fusion method, in obtaining high quality tracker output with greatly reduced input/output false alarm rates and communication throughput requirements. The analysis is made using simulated data for a multistatic sonar scenario from the Multistatic Tracking Working Group (MSTWG) [4].

Section 2 describes the SPECSweb concept and the high strength specular detection opportunities which provide the initial cues for further data retrieval. The data from the simulated multistatic scenario is also introduced. Section 3 describes the SPECSweb multistatic fusion and tracking algorithm. Section 4 provides results of the algorithm, applied to the simulated data set. Section 5 provides conclusions.

## 2. The Specular Detection Cue and Simulated Multistatic Scenario

The SPECSweb system concept is based on the exploitation of a target's high strength specular echoes, which occur when a sonar source and receiver are positioned with symmetric angles around the beam aspect of the target. When this specular condition occurs, it will yield a very high-strength target echo relative to other geometries, as indicated by the representative target strength function shown in figure 1. Consider a simulated multistatic scenario [5] from the MSTWG (provided by NATO Undersea Research Centre), as shown in figure 2. Three ships (red, blue, and green) are heading east, in-line, with an inter-ship spacing of approximately 13 km at 5kts. The target trajectory is shown to the north of the assets (in black) and heading west at 4kts. There are four multistatic nodes (source/receiver pairs) consisting of:

# Report Documentation Page

*Form Approved*
*OMB No. 0704-0188*



| 1. REPORT DATE | 2. REPORT TYPE | 3. DATES COVERED |
|---|---|---|
| **JUL 2008** | | **00-00-2008 to 00-00-2008** |

| 4. TITLE AND SUBTITLE | 5a. CONTRACT NUMBER |
|---|---|
| **Multistatic Target Tracking Using Specular Cue Initiation and Directed Data Retrieval** | 5b. GRANT NUMBER |
| | 5c. PROGRAM ELEMENT NUMBER |
| 6. AUTHOR(S) | 5d. PROJECT NUMBER |
| | 5e. TASK NUMBER |
| | 5f. WORK UNIT NUMBER |
| 7. PERFORMING ORGANIZATION NAME(S) AND ADDRESS(ES) **SPAWAR Systems Center San Diego,(SSC-SD),53560 Hull Street,San Diego,CA,92152-5001** | 8. PERFORMING ORGANIZATION REPORT NUMBER |
| 9. SPONSORING/MONITORING AGENCY NAME(S) AND ADDRESS(ES) | 10. SPONSOR/MONITOR'S ACRONYM(S) |
| | 11. SPONSOR/MONITOR'S REPORT NUMBER(S) |

12. DISTRIBUTION/AVAILABILITY STATEMENT
**Approved for public release; distribution unlimited**

13. SUPPLEMENTARY NOTES
**11th International Conference on Information Fusion, June 30 ? July 3, 2008, Cologne, Germany.**

14. ABSTRACT
**see report**

15. SUBJECT TERMS

| 16. SECURITY CLASSIFICATION OF: | | | 17. LIMITATION OF ABSTRACT | 18. NUMBER OF PAGES | 19a. NAME OF RESPONSIBLE PERSON |
|---|---|---|---|---|---|
| a. REPORT **unclassified** | b. ABSTRACT **unclassified** | c. THIS PAGE **unclassified** | **Same as Report (SAR)** | **8** | |

-Node 1: Source (ship 1)– Receiver (ship 1), monostatic
-Node 2: Source (ship 1) – Receiver (ship 2), bistatic
-Node 3: Source (ship 3) – Receiver (ship 1), bistatic
-Node 4: Source (ship 3) – Receiver (ship 2), bistatic
Note: there is no source on ship 2 and no receiver on ship 3.

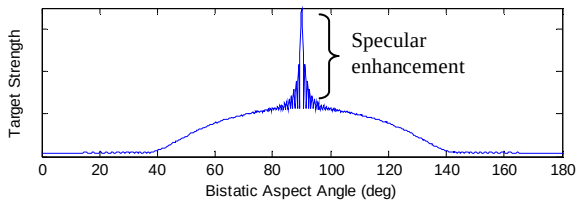


Figure. 1. Target strength as a function of bistatic aspect angle showing the high-strength specular peak (at 90 º).

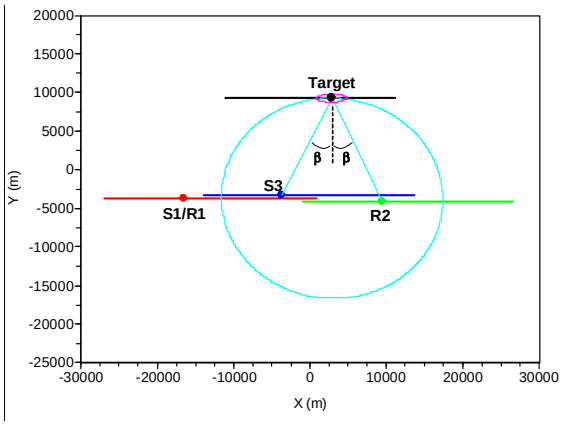


Figure. 2. The MSTWG NURC simulated multistatic sonar scenario at the time of the first specular for node 4 (Source 1 – Red; Receiver 1 – Red; Source 3 – Blue; Receiver 2 – Green; Target – Black).

The first specular opportunity during the scenario occurs for node 4, when source 3 and receiver 2 are positioned with equal, symmetric angles (β) from the target's beam aspect angle, as shown in the figure 2. Also shown is the bistatic equi-time ellipse (in cyan), and the specular detection's positional error ellipse (in magenta). Each receiver employs a towed array, which provides a bearing measurement for each sonar contact. The scenario duration is 180 minutes, with both sources transmitting FM waveforms every minute. There are a total of 720 scans of data in the scenario (4 per min).

Figure 3 shows the simulated contact data for a single node and a single ping transmission in geographic space. There are 200 contacts shown; one (unidentified) which originates from the simulated target; the other 199 are simulated false alarms. False alarm contacts are Rayleigh distributed in amplitude and uniformly distributed in measurement space. Figure 4 shows the simulated target detection SNRs corresponding to the four source-receiver combinations, for each of the 180 ping times. Note the slowly varying levels with large ping-to-ping fluctuations. Also notice the very high strength acoustic echoes corresponding to specular events (except for node 1), around pings 70, 95, and 117. By setting a higher-than-normal threshold setting (HTH), we can reject most of the scenario's false alarm clutter, while still detecting the specular echoes (as indicated in the figure). These specular contacts initiate tracks, and are used as cues to retrieve the additional detection data available on the other sensors in the multistatic field. The retrieved data from other sensors are referred to as "snippets", because they will be small subsets of the complete data which has been processed and stored on each of the local sensor nodes.

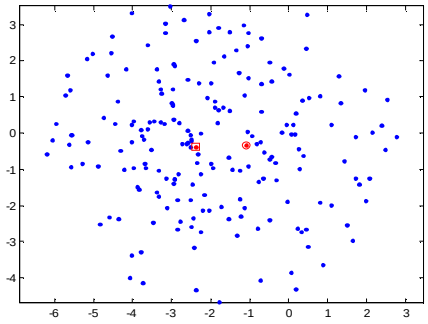


Figure. 3. The MSTWG NURC simulated multistatic sonar contacts for a single sonar node and single ping, in geographic space.

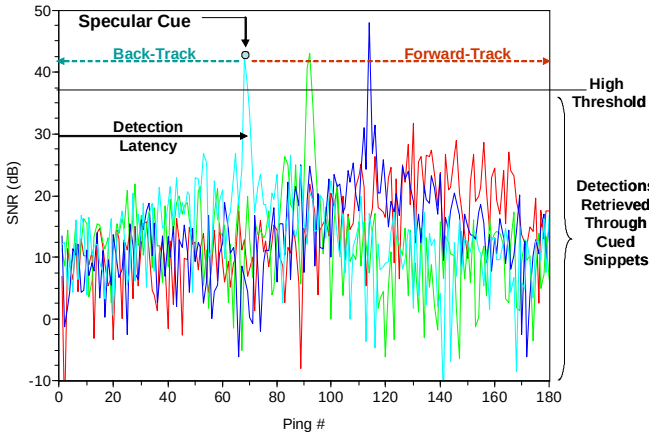


Figure 4. Target contact SNR vs. Ping number for the 4 multistatic sonar nodes (Node 1 - Red; Node 2 - Green; Node 3- Blue; Node 4 - Cyan).

A snippet's boundary and size is related to the specular cue measurement's area of uncertainty. Once a snippet has been identified and retrieved, the normal-level lower detection threshold (LTH) is applied within it, to identify additional potential target echoes. These are then passed over the communication link to a fusion center, as shown in figure 5. A track is initiated and the track's target state estimates (and projections) are used as the cues for subsequent measurements.

Using this scheme detection contacts can be retrieved for past and future pings, and tracks can be generated, both forward and backward in time. Such a cueing approach allows for a reduction in the amount of data which would normally be input into the fusion-tracking algorithm, enabling it to generate fewer false tracks. The main advantage of this approach is to greatly reduce the false alert rate, sensor communications requirements, and operator loading. The concept assumes that there will be a statistically sufficient number of specular occurrences to detect and initiate tracks. It also assumes that the increased detection

latency (needed to wait for specular detection opportunities to occur) is within the surveillance operation's reporting timeframe requirements. Evaluation metrics for studying the occurrence statistics of specular detection in multistatic fields have been developed [6].

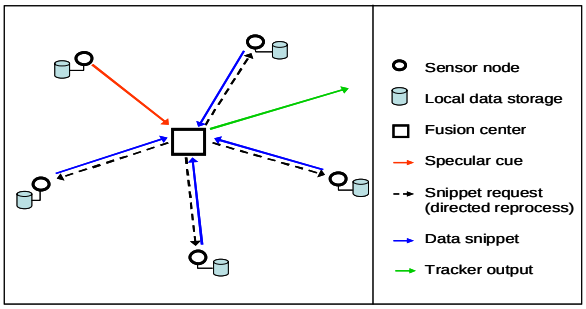


Figure 5. Diagram of the cueing concept.

## 3. SPECSweb Algorithm Description

The data model for the SPECSweb tracking algorithm assumes that each source-receiver pair produces multiple "contacts" (corresponding to clustered echo energies) with measurements of time delay, τ (from ping transmit time) and bearing, θ, (from the receiver). In the bistatic geometry [7], the range of a contact from the receiver can be obtained by

$$r = \frac{c^2\tau^2 - \Delta^2}{2(c\tau - \Delta\cos\alpha)} \tag{1}$$

where Δ is the distance between the source and receiver, α is the difference between the angle from the receiver to the target (θ), and the angle from the receiver to the source. $c$ is the speed of sound in water. Using this range and the bearing, the contact measurements may be mapped into an x-y position, in Cartesian coordinates. Contacts whose amplitudes exceed the low threshold (LTH) but not the high cue threshold (HTH) will provide measurements of target state position as

$$Z_{LTH} = \begin{bmatrix} x^m & y^m \end{bmatrix}^T. \tag{2}$$

This use of Cartesian measurements introduces a bias error in localization. A method for de-biasing bistatic Cartesian measurements has been derived [3], and is incorporated into the SPECSweb algorithm. We assume that the measurements have uncertainty errors with standard deviations as listed in Table 1.

Starting with these measurement errors, and using the analytic localization expressions derived in [8,9], the errors in contact localization in Cartesian coordinates ($\sigma_x$, $\sigma_y$, and $\sigma_{xy}$) can be obtained. The measurement error covariance matrix is then expressed as:

$$R_{LTH} = \begin{bmatrix} \sigma_x^2 & \sigma_{xy} \\ \sigma_{xy} & \sigma_y^2 \end{bmatrix}. \tag{3}$$

Table 1. Measurement errors.

| | |
|---|---|
| Arrival time | $\sigma_\tau$ |
| Bearing | $\sigma_\theta$ |
| Array heading | $\sigma_\phi$ |
| Speed of Sound | $\sigma_c$ |
| Source position | $\sigma_{x^S}$, $\sigma_{y^S}$, *and* $\sigma_{x^S y^S}$ |
| Receiver position | $\sigma_{x^R}$, $\sigma_{y^R}$, *and* $\sigma_{x^R y^R}$ |

Contacts whose amplitudes exceed the high cue threshold (HTH) are assumed to be specular echoes, and in addition to a target position measurement, a target heading measurement is obtained. Targets in the specular condition have a heading which is tangential to the bistatic equi-range ellipse at the contact location. There will be an ambiguity between two heading assumptions; one clockwise and one counter-clockwise (180 degrees out of phase) about the ellipse at this point of tangency. In this case, the measurement provides both positional and heading information in the target state as

$$Z_{HTH} = \begin{bmatrix} x^m & y^m & \dot{x}^m & \dot{y}^m \end{bmatrix}^T \tag{4}$$

where $x^m$ and $y^m$ are the same as before and

$$\dot{x}^m = v_T \cdot \cos H \tag{5}$$

$$\dot{y}^m = v_T \cdot \sin H \ , \tag{6}$$

where $v_T$ is the assumed or estimated target speed and H is the target heading corresponding to the specular condition. We assume the uncertainty in the target speed and specular heading are given by $\sigma_{v^T}$, and $\sigma_H$, respectively. Following the same small-error linearization method described in [8,9], errors in target velocity can be derived. The velocity errors in Cartesian coordinates are given as

$$\sigma_{\dot{x}}^2 = \sigma_{v^T}^2 \cos^2 H + \sigma_H^2 v^{T^2} \sin^2 H \tag{7}$$

$$\sigma_{\dot{y}}^2 = \sigma_{v^T}^2 \sin^2 H + \sigma_H^2 v^{T^2} \cos^2 H \tag{8}$$

$$\sigma_{\dot{x}\dot{y}} = (\sigma_{v^T}^2 - \sigma_H^2 v^T) \sin H \cos H \tag{9}$$

The measurement error covariance for this case is then given as the following 4x4 matrix

$$R_{HTH} = \begin{bmatrix} R_{LTH} & 0_{2,2} \\ 0_{2,2} & R_v \end{bmatrix}, \text{ where} \tag{10}$$

$$R_v = \begin{bmatrix} \sigma_{\dot{x}}^2 & \sigma_{\dot{x}\dot{y}} \\ \sigma_{\dot{x}\dot{y}} & \sigma_{\dot{y}}^2 \end{bmatrix} \tag{11}$$

In the case when a current target speed estimate is unavailable (as in the case of a track initiating specular cue), an initial value and uncertainty of the target speed is assumed.

The target is modeled assuming a 2-dimensional *nearly constant velocity* motion model [10]. It allows for maneuvering through a process noise term, and has been shown to be effective in ASW tracking [2, 3] .

A logic-based track initiation and termination scheme is used. Scans from multiple sensors, occurring at the same (ping) time, are ordered in an arbitrary way. A track is initiated upon the successful association of contacts from M out of N successive scans of data where the first detection has exceeded the HTH. Track termination is made when K consecutive scans of data are processed without providing associable contacts.

The SPECSweb tracking algorithm is implemented in Cartesian coordinates. Once a track has been initiated, subsequent updates to the track are made using the equations of the Kalman Filter [11]. Measurements above the LTH (but below the HTH) and selected for association will update the track using only positional measurements and error covariance. Cue measurements above the HTH will first be associated to existing tracks, if possible, otherwise they will initiate new tracks. If updating a track, the cue measurement will provide both target position and target heading information.

Data associations between existing tracks and new measurements are made using the statistical "nearest neighbor" method. The tracks are ordered according to length, with longer tracks getting priority over shorter tracks for new association assignments. Only "validated" contacts are considered for association to existing tracks. Validated contacts are those that are fall within a suitable association gate and which exceed the low threshold (LTH). We use a two-dimensional ellipsoidal association gate [12]. A method for determining the data retrieval snippet boundaries corresponding to this gating scheme is given in [13]. The gating (or snippet) size may be scaled to achieve a desired level of association probability. The contact with the highest association probability (nearest statistical neighbor) within the snippet is used to update the track. Once a contact has been assigned to a confirmed track, it becomes unavailable for association to other tracks. Only validated contacts need to be retrieved and sent over the communications link for fusion, greatly reducing multistatic communication throughput requirements.

The SPECSweb tracking algorithm flow is shown in figure 6. Scans of data are sequentially processed, searching for cues (contacts exceeding the HTH). Once a cue is obtained, two tentative tracks are declared, corresponding to the two specular heading assumptions. Next, contacts contained within snippets are retrieved from other sensors and previous pings, for possible association and reverse-time track update. After the M/N criterion is met, backtracks become confirmed. Reverse-time tracking continues, in order to capture as much track history as possible. Once the two backtracks have both terminated, the more probable backtrack is selected, using track length and heading stability criteria. The contacts belonging to the correct backtrack are then re-filtered in the forward-time direction, until the current time (of the initiating specular cue) is reached. With this re-filtering, the best possible track estimate at the time of the cue is obtained. At this point the track continues in the forward-time direction updating with measurements found within the retrieval snippets of future scans. Subsequently occurring specular detections update track position and heading, if they are determined to be the nearest neighbor contact in the snippet. Specular detections which are not assigned to existing tracks become new tentative tracks, and the process repeats. Current forward-direction tracks will terminate when the termination criterion is met.

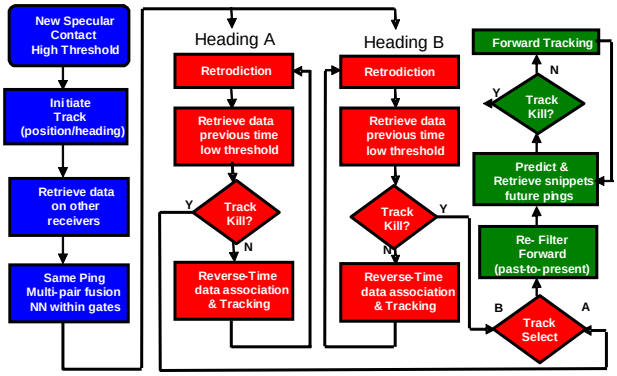


Figure 6. SPECSweb tracker flow chart.

## 4. SPECSweb Tracking Results for MSTWG NURC Simulation Scenario

The SPECSweb tracking algorithm was applied to the MSTWG NURC data with input parameters set as listed in Table 2. The specular threshold (HTH) has been optimally chosen to detect the first specular event, and the low threshold has been set to provide an input probability of detection of about 0.7 along with all 796 false contacts per minute (full set of false contacts ingested).

Figure 7 shows the tracker output after the entire scenario has been processed. Despite the high clutter rate, the SPECSweb tracker shows excellent performance with a single high quality target track (plotted in red) corresponding to the target's true trajectory (in yellow). There are zero false tracks generated. Figure 8 shows a zoomed view of the tracker output. Here, the three specular detections are overlaid on the track. The track piece to the right of the specular cue was backtracked, and then re-filtered in the forward direction. This was then stitched to the forward track, which correctly associated the 2nd and 3rd specular detections with the track. The detection latency of the target was 67 minutes (the time after scenario start time to the 1st cue occurrence). At this time however, a full track history (of 67 minutes) was made available. Though for this scenario the target is nearly non-maneuvering, the algorithm is capable of tracking targets through maneuvers through use of the nearly constant velocity motion model.

Table 2. Tracker Input Parameters.

| | |
|---|---|
| Track initiation (M of N scans) | 1/1 |
| Track termination (K scans) | 7 |
| Association Gate Probability | 99% |
| Cue Threshold (HTH) | 38 dB |
| Low Threshold (LTH) | 10 dB |
| Maneuverability index ($m^2/s^3$) | 0.001 |
| Initial guess target speed | 4 kts |
| Error of initial target speed | 2 kts |
| Error of source/receiver positions | 10 m |
| Error of receiver bearing | 2° |
| Error of receiver timing | 0.01 s |
| Error of speed of sound | 15 m/s |
| Error of specular heading | 10° |

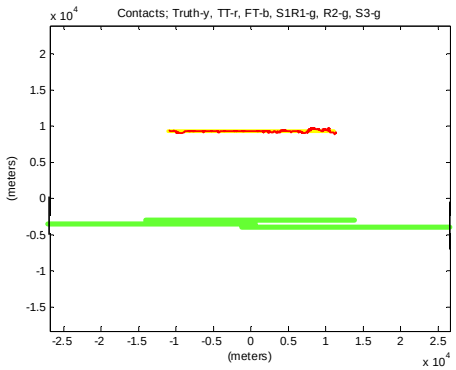


Figure 7. SPECSweb tracker results; ship/asset true trajectories (green), target true trajectory (yellow); tracker output (red).

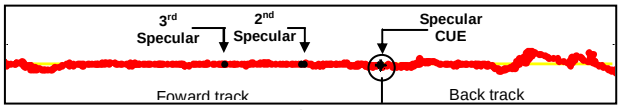


Figure 8. Zoomed view of the tracker output, showing the location of specular detections along the track.

Figure 9 shows the tracker input and output localization accuracy as a function of scan number. The filtering of measurements leads to a significant improvement (by a factor of 5) in the target localization accuracy. Figure 10 shows the heading and speed estimates obtained by the tracker, as a function of scan number. These show good agreement with the actual target values (heading of 180° and speed of 2 m/s), except at the very beginning of the track. Figure 11a shows the two backtrack segments, one for each of the two specular heading assumptions. In this case they are nearly identical. In Figure 11b shows the correct backtrack with the forward re-filtering overlaid. Here we see some differences, but the forward filtered track produces the better track estimate at the time of the initiating cue for continued forward tracking.

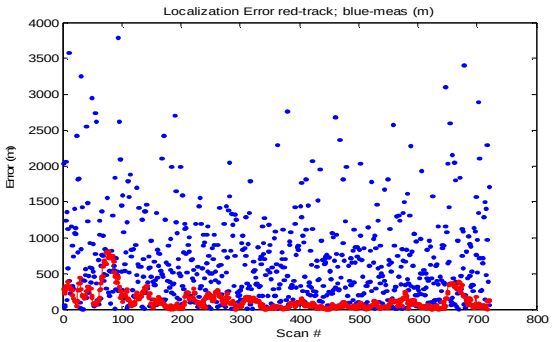


Figure 9. Tracker localization error; input data (blue), output track (red).

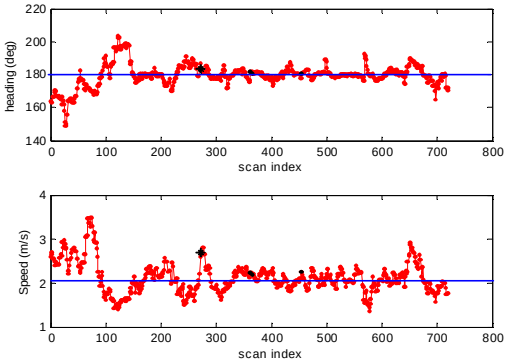


Figure 10. Tracker accuracy in heading and speed; truth (blue), tracker output (red).

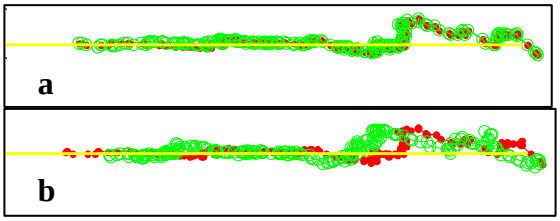


Figure 11. (a) Backtracks; heading 1 (red); heading 2 (green). (b) Correct backtrack (red); backtrack filtered forward in time (green).

The SPECSweb approach has a significant impact on the communication link load. This is because only cue data, snippet requests, and snippet data, need be sent over the link, instead of complete contact data. Assuming approximately 55 bytes are needed to describe a single contact [14], the required communications throughput for SPECSweb is reduced by more than two orders of magnitude (7920 to 35 Kbytes) for the entire scenario. The MSTWG tracker performance metrics [4] were calculated, and are shown in Table 3. The probability of detection (PD) is improved from 0.7 to 1.0, the false alarm rate (FAR) is decreased from 796/min to zero, and the localization is greatly improved.

To more completely characterize the performance of the tracker, we have evaluated the tracker under different input receiver operating characteristics (ROC) conditions. This was done by iteratively running the tracker and varying the LTH from -20 to +30 dB. For this analysis, we kept the cue threshold (HTH) fixed. This creates different conditions for the tracker: as the

threshold is raised, less data is available to the tracker, and the input PD and the FAR will decrease.

Table 3. Tracker Performance Statistics.

| | |
|---|---|
| Detection latency (min) | 67 min |
| PD - Input | 0.7 |
| PD - Output | 1.0 |
| FAR - Input | 796 / min |
| FAR - Output | 0 / min |
| Comms throughput (per scenario):<br>- Conventional (single LTH)<br>- SPECSweb (LTH/HTH) | <br>7920 KBytes<br>35 KBytes |
| Localization Error - Input | 682 m |
| Localization Error - Output | 132 m |
| Track Purity | 91% |
| Coasts | 25% |
| Fragmentation | None |
| Compute time (fraction of real time) | 0.01 |

Figure 12 shows the results in terms of PD at the input and output of the tracker, as a function of LTH. The circled (in green) points indicate the algorithm input operating points for the results already given in table 3. As the threshold is raised, the PD decreases, from one, to near zero. The increased PD performance of the tracker output compared to the input, is obtained because the tracker is able to maintain a track even when target detections are missed. Figure 13 shows the results for the false alarm rate (FAR) as a function of threshold. Raising the threshold to around 12-14 dB abruptly decreases the FAR at the input to the tracker. We see that the performance of the SPECSweb tracker is very good in reducing false tracks. In each and every case, the tracker outputs zero false tracks.

These results are combined into a ROC-style plot in figure 14. The best performance is obtained when operating in the upper left corner of the plot (zero false alarms and 100% PD). The blue and red curves show the tracker input and output ROC statistics, respectively, as the threshold was varied. Many of the target detections are below the levels of the false alarms, as indicated by the sharp rise in PD after the threshold drops enough. The output ROC curves shows perfect performance in reducing the false alarm rate to zero, and variable levels of performance in PD, depending on the input PD. A modified version of this ROC curve is shown in figure 15, where the input ROC points are connected to their corresponding output ROC points, by a line. Each run of the tracker (with different threshold) is represented by a separate line. Here the FAR performance can be visualized by how far the lines extend to the left, toward zero false alarms. The output PD should be equal to or better than the input, and this is shown to be the case with the lines sloped upwards toward higher PDs. Even in the case of full contact ingestion (LTH = -∞), the tracker is able to produce PD=1, and zero false tracks at the output.

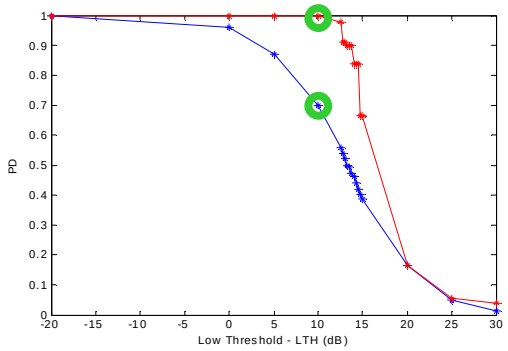


Figure 12. SPECSweb tracker input (blue) and output (red) PD as a function of low threshold (LTH). Circles indicate operating points for the results given in Table 3.

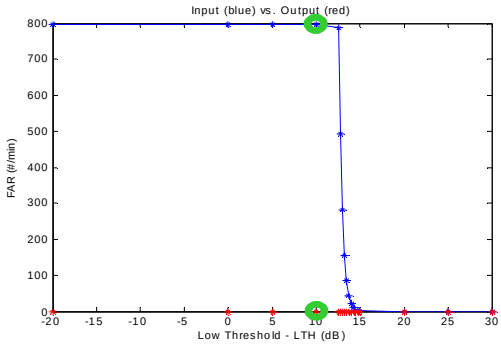


Figure 13. Tracker input (blue) and output (red) FAR as a function of variable low threshold (LTH).

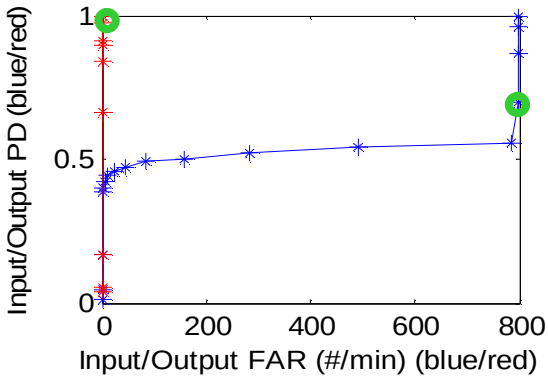


Figure 14. SPECSweb tracking input (blue) and output (red) ROC curves, as mapped out by variable LTH.

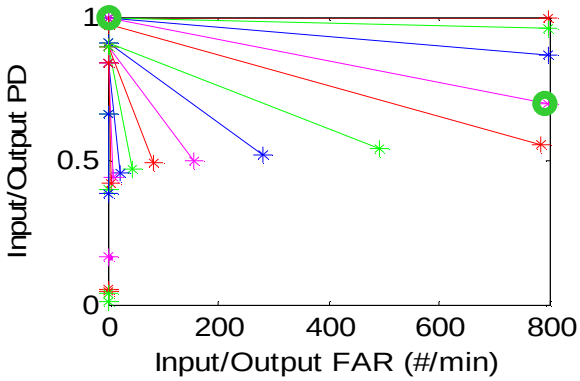


Figure 15. Alternate form of the ROC curves of figure 14, showing input/output ROC points for each LTH.

We now compare the SPECSweb tracking performance with a "conventional" tracking approach. The conventional tracker used here is similar to the SPECSweb tracker, except that it employs only a single threshold (LTH), both for track initiation and update. It does not utilize any specular heading information in the measurements, and it does not perform backtracking. It uses the same Cartesian data model, target motion model, and nearest neighbor data association as the SPECSweb tracker. Results are compared for cases when both algorithms provide an output (true) target track probability of detection (PD) level of 98%. The track initiation criterion for the SPECSweb tracker is taken to be M/N=1/1 (and exceeding the HTH), and for the conventional tracer it is M/N=3/4 (all exceeding the LTH). All other tracking parameters are kept the same.

Results of the two trackers are compared in Table 4. The SPECSweb approach shows superior performance in reducing the communications link loading, by about two orders of magnitude. The SPECSweb tracker outputs zero false tracks, while the conventional tracker suffers from an unacceptably high false track rate. The unloading feature of the SPECSweb tracker also results in much lower computation time (as measured on a standard PC) which is well within the real-time operational limits. The SPECSweb tracker performance is also somewhat better in localization errors and fragmentation. The detection latency is higher for the SPECSweb than the conventional algorithm, as it must wait for the 1st specular occur (around 1 hour, for this particular scenario). The conventional tracker produced two tracks on the target for this scenario; the first fragment after 2 minutes, the second after 19 minutes.

Figures 16 and 17 show the complete scenario contact sets which are used as input to the trackers, mapped in geographic space. These also represent the contact data which is required to be sent over communications links, from sensors to a centralized location where the tracking algorithms may be applied. Sonar source/receiver trajectories are shown in green. Figures 18 and 19 show the output of the trackers; true target tracks are shown in red, false tracks in blue. While the two trackers show equivalent performance in tracking the target (as the comparison was set up to do), the SPECSweb tracker clearly has superior performance in reducing communication link loading and false track rates.

Table 4. SPECSweb vs. Conventional Tracking

| Metric (output PD≈0.98) | SPECSweb (M/N=1/1) | Conventional (M/N=3/4) |
|---|---|---|
| Required Comms Throughput (scenario) | 30 KB | 2800 KB |
| Output FAR | 0 | 423/hour |
| True Track Fragments | 1 | 2 |
| Localization Error | 136 m | 146 m |
| Compute Time (fraction of real time) | 0.009 | 2.7 |
| Detection Latency | 67 min | 2 min (frag1)<br>19 min (frag2) |

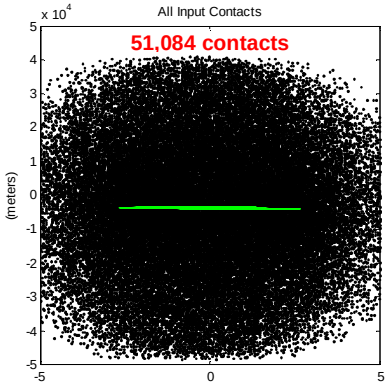

Figure 16. Required contacts sent over communications links and input to the conventional tracking algorithm.

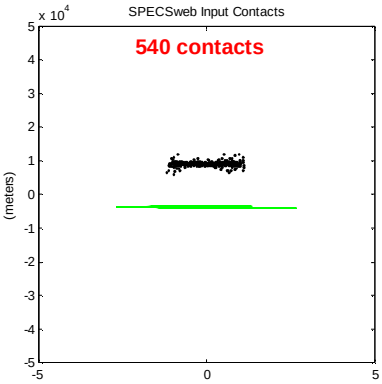

Figure 17. Required contacts sent over communications links and input to the SPECSweb tracking algorithm.

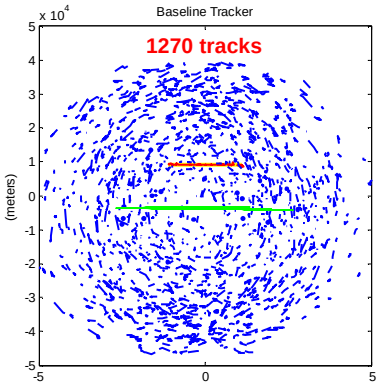

Figure 18. Conventional tracker output.

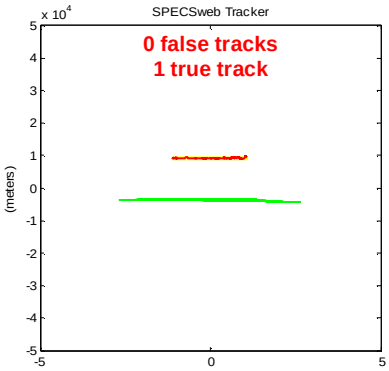

Figure 19. SPECSweb tracker output.

## 5. Conclusions

The SPECSweb tracking and fusion algorithm has been described. Its application to the MSTWG simulated data set shows excellent performance. The use of two thresholds has been demonstrated; the higher threshold (HTH) effectively exploits the specular echo as a cue for initiating a tracking process, and the lower threshold (LTH) for selective snippet retrieval and track update.

The results show that with sufficient PD at the input to the tracker, a single high quality target track results. In all cases tested, there were zero false tracks output by the algorithm. In the specific case shown, the algorithm was very effective at reducing the fusion input data rate from 796 contacts/min to 4 contacts/min. This corresponds to a reduction in communications link loading of 7920 Kbytes down to 35 Kbytes for the scenario. For this scenario the track detection latency was about 1 hour, but a complete track history was available at that time. The algorithm performance was shown to be effective over a range of LTH values, as characterized by ROC curves.

The SPECSweb algorithm was also compared to a conventional, single threshold tracking algorithm. This showed that the SPECSweb approach effectively provided the unloading and false alarm reduction performance we seek, and which were not attainable using the conventional approach. The SPECSweb results also compare extremely favorably with other tracking approaches that have been applied to this same MSTWG data set (with excellent output ROC metrics, at the expense of additional latency), as reported in [15].

Future work will focus on more parametric evaluation, application to other simulated and real multistatic datasets, and the incorporation of Doppler and target classification information.

## Acknowledgements

This work was sponsored by the Office of Naval Research, 321 US.

The concept of specular cueing for multistatic systems was originally developed and modeled by Shelby Sullivan Sr. (APL/UW) and James Alsup (SAIC) in the late 1990's under the sponsorship of the Office of Naval Research.

## References

[1] D. Grimmett and S. Coraluppi, Multistatic Active Sonar System Interoperability, Data Fusion, and Measures of Performance, NURC Technical Report NURC-FR-2006-004.

[2] S. Coraluppi and D. Grimmett, Multistatic Sonar Tracking, in Proceedings of the SPIE Conference on Signal Processing, Sensor Fusion, and Target Recognition XII, April 2003, Orlando FL, USA.

[3] S. Coraluppi and C. Carthel, Progress in Multistatic Sonar Localization and Tracking, SACLANTCEN Report SR-384, December 2003.

[4] S. Coraluppi, D. Grimmett, and P. de Theije, Benchmark Evaluation of Multistatic Trackers, in Proceedings of the 9th International Conference on Information Fusion, July 2006, Florence, Italy.

[5] D. Grimmett and S. Coraluppi, Contact-Level Multistatic Sonar Data Simulator for Tracker Performance Assessment, in Proceedings of the 9th International Conference on Information Fusion, July 2006, Florence, Italy.

[6] D. Grimmett, S. Sullivan, Sr., and J. Alsup, Modeling Specular Occurrence in Distributed Multistatic Fields, in Proceedings of the IEEE OCEANS'08 Conference, July 2008, Kobe, Japan.

[7] H. Cox, Fundamentals of Bistatic Active Sonar, in Underwater Acoustic Data Processing, Kluwer Academic Publishers, 1989.

[8] S. Coraluppi, Multistatic Sonar Localization, IEEE Journal of Oceanic Engineering, Vol. 31, No. 4, October 2006.

[9] S. Coraluppi, Multistatic Sonar Localization Analysis, NURC Technical Report SR-377, June 2003.

[10] Y. Bar-Shalom and X. Li, Estimation and Tracking: Principles, Techniques, and Software, Norwood, MA: Artech House, 1993, Chap 6.

[11] M. Grewal and A. Andrews, Kalman Filtering Theory and Practice, Englewood Cliffs, NJ: Prentice Hall, 1993.

[12] S. Blackman and R. Popoli, Design and Analysis of Modern Tracking Systems, Norwood, MA: Artech House, 1999, ch. 6.3.

[13] D. Grimmett, Reduction of False Alarm Rate in Distributed Multistatic Sonar Systems through Detection Cueing, Proceedings of the IEEE Oceans'07 Conference, June 2007, Aberdeen, Scotland.

[14] R. Laterveer, Contact File Format, NURC Technical Memo, RL-MAR05, March 2005.

[15] D. Grimmett, S. Coraluppi, B. La Cour, C. Hempel, T. Lang, P. de Theije, and P. Willet, MSTWG Multistatic Tracker Evaluation Using Simulated Scenario Data Sets, in Proceedings of the 11th International Conference on Information Fusion, July 2008, Cologne, Germany.